Received: 5 March 2022 | Revised: 17 May 2022 | Accepted: 19 May 2022

DOI: 10.1002/jhet.4520

ARTICLE

JOURNAL OF HETEROCYCLIC CHEMISTRY WILEY

Synthesis and molecular modeling of some novel hydroxypyrone derivatives as antidermatophytic agents

Gülşah Karakaya[1] | **Aslı Türe**[2] | **Aysun Özdemir**[3] | **Berrin Özçelik**[4] | **Mutlu Aytemir**[1,5]

[1]Faculty of Pharmacy, Department of Pharmaceutical Chemistry, İzmir Katip Çelebi University, İzmir, Turkey

[2]Faculty of Pharmacy, Department of Pharmaceutical Chemistry, Marmara University, İstanbul, Turkey

[3]Faculty of Pharmacy, Department of Pharmacology, Gazi University, Ankara, Turkey

[4]Faculty of Pharmacy, Department of Pharmaceutical Microbiology, Gazi University, Ankara, Turkey

[5]Faculty of Pharmacy, Department of Pharmaceutical Chemistry, Hacettepe University, Ankara, Turkey

Correspondence
Gülşah Karakaya, Faculty of Pharmacy, Department of Pharmaceutical Chemistry, İzmir Katip Çelebi University, İzmir, Turkey.
Email: gulsah.karakaya@ikc.edu.tr

Funding information
Gazi Üniversitesi, Grant/Award Number: 02/2011-35; Türkiye Bilimsel ve Teknolojik Araştirma Kurumu, Grant/Award Number: SBAG113S527

Abstract

Dermatophytes are pathogenic fungi, comprising the major cause of superficial fungal infections called dermatophytes. Although they infect keratinized tissues such as skin, nail, and hair, invasive serious infections may occur in immunocompromised patients. However, current antifungal drugs show considerable drawbacks, such as toxicity and multiple drug resistance, compelling and directing researches for new antidermatophyte agents. Herein, a series of hydroxypyrone bearing compounds inspired from the natural metabolite kojic acid was reported. Their antidermatophytic effects of the compounds against *Microsporum gypseum, Trichophyton mentagrophytes var. erinaceid*, and *Epidermophyton floccosum* were evaluated. The cytotoxicity of the compounds on healthy (MRC-5) and carcinogenic (He-La) cell lines was also investigated, and their cytopathogenic effects were expressed as maximum non-toxic concentrations. According to the activity studies, compounds **10** and **22** were found as the most promising antidermatophytic agents (MIC: 2 μg/ml), exhibiting comparable effect with that of griseofulvin (MIC: 0.5–1 μg/ml) and terbinafine (MIC: 0.125–0.5 μg/ml) which are the most widely used agents for treating mycoses caused by dermatophytes. Molecular docking analysis of the most active compounds, compound **10** and compound **22**, with homology model of β-tubulin protein was carried out to investigate the possible binding conformation of the compounds in the targeted macromolecule.

1 | INTRODUCTION

Many people and animals suffer from superficial infections known as dermatophytoses, caused by a group of pathogenic highly specialized filamentous fungi called dermatophytes [1]. Due to the growing prevalence of fungal infections, dermatophytoses have become one of the most commonly distributed infections worldwide. Although dermatophyte infections are generally restricted to the surface of keratinized structures such as nails, skin, and hair, the fungi can be invasive and cause serious widespread and even life-threatening infections depending on the amplitude of the infection and the immune status of the host [2].

Dermatophytes consist of three genera, including *Trichophyton*, *Microsporum*, and *Epidermophyton* according to the formation and morphology of their conidium [3]. Among the species, *T.rubrum* is the leading cause of human skin and nail mycoses and also has high prevalence [4]. Dermatophytes require the cleavage of keratin to gain nutrients for their survival, so they produce lytic enzymes to hydrolize proteins and uptake released nutrients [5].

Although there is a reasonable number of antifungal drugs commercially available, these act on a limited

number of cellular targets. These drugs are effective on the plasma membrane, cell wall, nucleic acids, and the cell division process [6]. Currently, cytochrome P450 sterol 14α-lanosterol demethylase, β-tubulin, chitin synthase, squalene epoxidase and β-1,3-glucan synthase enzymes can be stated as the main targets of antifungal agents. For instance, azole derivative drugs like itraconazole, fluconazole, posaconazole, voriconazole etc. are 14 α-lanosterol demethylase inhibitors. Allylamine derivative agents like terbinafine and naftidine inhibit squalene epoxidase enzyme, both leading to inhibition of ergosterol synthesis. The very well-known antifungal agent griseofulvin interferes with microtubule assembly and inhibits mitosis by interacting with tubulin protein, impairing fungal growth and cell-division [7] (Figure 1).

Current therapeutic options used for dermatophytosis are still limited due to high toxicity, poor efficacy, drug interactions, and antifungal resistance due to the similarity that exists between fungi and host cells. Multidrug resistance also occurs because of overlapping mechanisms of action of the commonly used drugs intensifying the prospect of successful treatment. Therefore, it is imperative to develop new agents with safer profiles and having specific modes of action so as to make synergism in drug combinations.

Natural products have served as a research tool for drug discovery and inspired the production of synthetic therapeutic agents, providing a basis for chemical research. Kojic acid (5-hydroxy-2-hydroxymethyl-4*H*-pyran-4-one, KA), is one of the natural metabolite produced by many species *Aspergillus*, *Acetobacter*, and *Penicillium* in an aerobic process from a wide range of carbon sources [8]. KA and its derivatives attract more attention due to multiple bioactivities [9–15].

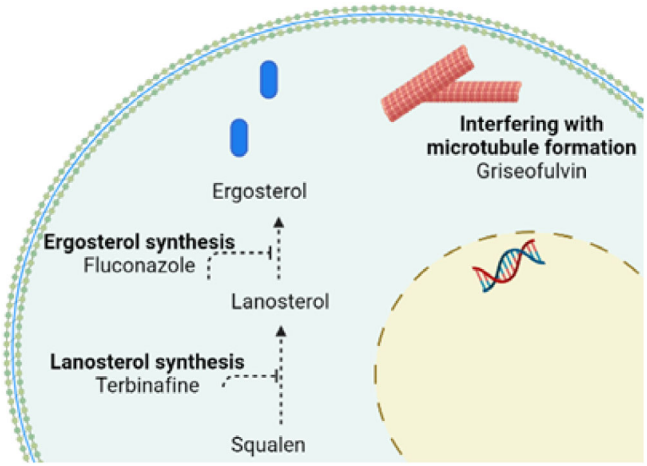

FIGURE 1 Currently used antidermatophytic drugs and their mode of actions.

In our previous studies, antifungal activities of KA derived compounds guided us for further studies [10, 11]. Mannich bases of chlorokojic acid (2-chloromethyl-5-hydroxy-4*H*-pyran-4-one), produced by chlorination of the alcoholic hydroxyl group, were prepared and their antitubercular [16] and antidermatophytic properties were screened [17]. In a follow-up work, the biological activity of some novel KA derivatives bearing dichlorobenzyl piperazine moieties including antityrosinase, antiaging, antimycobacterial, antidermatophytic, and antioxidant activities was patented with the title of "Kojic Acid-Derived Mannich Bases with Biological Effect" [18]. However, interactions with possible targets at fungal cell were nondiscussed.

Therefore, as a part of our long-term efforts to find novel candidates having improved bioactivity and low cytotoxic effect, herein, Mannich bases of kojic acid were synthesized. Heterocyclic amines have emerged as excellent templates for various bioactive molecules with antifungal properties. To give some examples, piperazine ring, a core structure of many marketed drugs, often shows increased antimicrobial activity attributed to its ability to enhance lipophilicity of the compound [19]. As a saturated heterocyclic, piperidine also reported for its multiple activities including antifungal activity [20]. In addition, tetrahydropyridine is a structural part of many synthetic pharmacologically active molecules as the main pharmacophore as well as a substituent with its known antimicrobial and antifungal effects [21]. In the light of those data, at present work, piperazine, piperidine, and tetrahydropyridine structures were used as secondary amines to gain Mannich bases.

Their antidermatophytic effects against *Microsporum gypseum, Trichophyton mentagrophytes var. erinaceid*, and *Epidermophyton floccosum* and cytotoxic features at nontoxic concentrations on MRC-5 and He-La cell lines were evaluated by using broth microdilution methods. To achieve more molecular insight, modeling studies were performed to estimate the possible binding conformation of the compounds on the literally known target, the amino acids sequence of tubulin β-subunit of *T. rubrum*. In attempt to expose a comprehensive structure–activity relationships and to make explication of the results with our previous studies, some analogues of Mannich bases, reported before [12, 22, 23], were included in the current study and their antidermatophytic effects with cytotoxicities were presented for the first time.

Overall; synthesis, antidermatophytic activity, and molecular modeling results of 25 Mannich bases of kojic acid comprising 11 novel agents were studied and presented here.

2 | RESULTS AND DISCUSSION

2.1 | Chemistry

The rapid development of molecular diversity is an important goal of organic and medicinal chemistry to achieve more insight in drug discovery studies. Multicomponent reactions (MCRs), in which three or more reactants joined to form the required product in a one-pot procedure, are beneficial methods. Mannich reactions are among the most important MCRs that form carbon–carbon bonding and provides structural diversity. It is a three-component condensation reaction involving an active hydrogen-containing compound, formalin, and a secondary amine. Additionally, these reactions have many advantages ranging from lower reaction times, increased reaction rates to higher yields and reproducibility [24]. Also, increasing the lipophilicity of the compounds by gaining Mannich bases is a well-known method [11, 16] with the substitution of different lipophylic aryl derivatives and bulky groups at the cyclic amines. This ability is also a critical feature of substances used in the treatment of superficial mycoses to ease their penetration in to the stratum corneum and persist at a constant concentration throughout the therapy [5].

Since KA contains a polyfunctional hydroxypyrone ring with several important centres enabling additional reactions, herein different amine fragments including substituted piperazine, tetrahydropyridine, and piperidine groups were introduced to the structure. In the present work, 25 compounds having structure of 6-hydroxymethyl-3-hydroxy-2-(substituted piperazine/tetrahydropyridine/piperidine-1-yl)methyl-4*H*-pyran-4-one including 11 new agents, were synthesized by the Mannich reaction with KA in the presence of formaline. The synthetic route of the target compounds is shown in Figure 2. The one-pot reaction was carried out in mild conditions and rapidly proceeded with high yields at room temperature.

The structures of the novel compounds were verified by using spectroscopic techniques and elemental analysis results. The yields of the reactions and melting points were given in monographs. The related documents can be found in Appendix S1.

The selected diagnostic bands of the IR spectra of compounds provided useful information for determining the hydroxypyrone skeleton. Hydroxymethyl moiety showing two hydrogen bondings, both intra- and intermolecular, C=O (pyranone) stretching gave signals at 1617–1597 cm^{-1}. In the IR spectra of all compounds, the stretching (st) bands associated with C=C and C−O were observed at about 1467–1443, and 1201–1187 cm^{-1} respectively. The formation of the novel Mannich bases

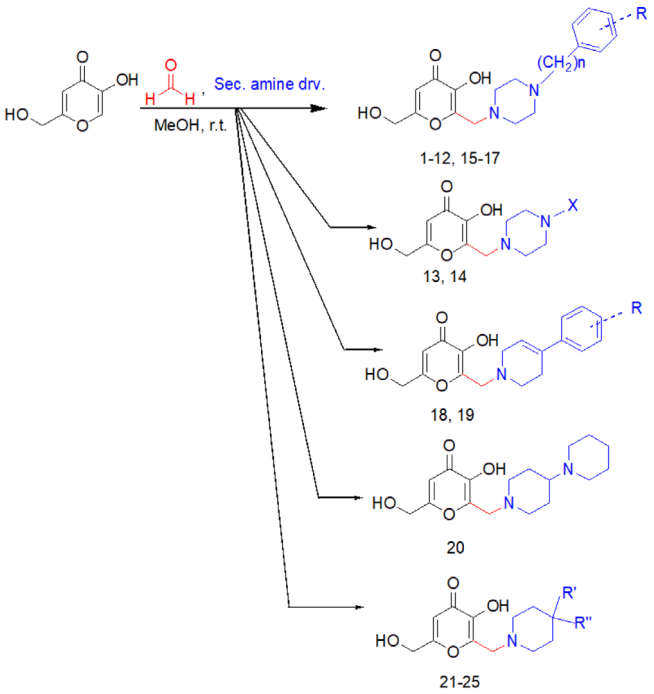

FIGURE 2 General synthesis of compounds **1–25**.

of kojic acid was further confirmed with the ^{1}H NMR spectra based on the chemical shifts and intensity pattern. Characteristic singlet peaks of the 4*H*-pyran-4-one (H^5) ring proton were found in the region 6.29–6.34 ppm per the literature [16, 17]. Aromatic hydrogens of phenyl rings were at 6.81–7.55 ppm with suitable integral values. The other -CH_2- group proton signals also appeared as singlet peaks at 3.49–3.59 ppm. The ^{13}C NMR signals of compounds were in good agreement with proposed structures. All the compounds displayed characteristic peaks of methylene group (CH_2-OH) carbons at 109 ppm. The carbon atom linked to the hydroxyl group on the third position of the pyranone ring (=*C*-OH) exhibited signals at 151–154 ppm. Signals between 48 and 60 ppm were due to carbons of *piperazine* rings, whereas the range 50–54 ppm belongs to *tetrahydropyridine* carbons. Carbons of aromatic phenyl rings were observed at about 116–147 ppm. Carbonyl carbons of the 4*H*-pyran-4-one ring were found at 174 ppm. The distinctive signals of the compounds were observed in the mass spectra that followed a similar fragmentation pattern. The entire spectrums showed molecular ion peaks and M^{+}+23 (Na) peaks.

2.2 | Bioactivities

Interests in discovering new antimicrobials effective to pathogenic bacteria and safe for healthy cells of the

human body have a long history. Still, recently this has been growing faster among many fields. However, the problem of antibiotic resistance to multiple versions of drugs caused by excessive and uncontrolled intake of antibiotics has been a major global concern. Therefore, beyond existing antimicrobial agents, newly designed compounds, which may have valuable new targets with improved biological effects and none/less cytotoxicity, are needed.

The three major classes of antifungal drugs used to treat dermatophytoses are the allylamines, azoles, and griseofulvin. The azoles inhibit sterol 14 α-demethylase, while allylamines inhibit squalene epoxidase; both leading to the inhibition of ergosterol biosynthesis which causes the accumulation of toxic sterol precursors, reducing cell membrane function and fungi growth. Griseofulvin impairs fungal growth and cell division by interfering with microtubule formation [25]. In the present study, terbinafine, itraconazole, and griseofulvin were used as standard agents as representative drugs of those classes respectively for in vitro investigation of antidermatophytic activity by using the broth microdilution method. Also, the cytotoxicity of all Mannich bases was determined by using eukaryotic cells (He-La, MRC-5) under the maximum nontoxic concentrations (MNTCs: ≥128 to ≥256 μg/ml).

The structures of Mannich bases synthesized in the scope of this study can be evaluated in terms of possessing secondary amines into three groups: piperazine, tetrahydropyridine, and piperidines. Many of these compounds carry mono- or di-substituents on their aromatic rings, including halogen atoms, methyl, methoxy, or acetyl groups. As exceptions, compounds **13** and **14** bearing cyclohexyl and cyclohexanecarbonyl piperazine moieties instead of phenyl or benzyl groups have no substitutions on the rings.

All the compounds exhibited good antidermatophytic potency with MIC values between 2 and 32 μg/ml against both standard and isolated strains of *Microsporum gypseum, Trichophyton mentagrophytes var. erinacei*, and *Epidermophyton floccosum*. As shown in Table 1, compound **10** with 4-chlorophenyl piperazine ring and compound **22** with 4-(4-bromophenyl)-4-hydroxypiperidin-1-yl exhibited the highest activity against three dermatophytes species (MIC: 2 μg/ml). The distinctive structural property of this compound has electronegative halogen substituent on the 4th position of the aromatic ring. 2- or 3-chlorophenyl carrying compounds (compounds **8** and **9**) also have MIC values of 4–8 μg/ml against all dermatophytes. In addition to this, when compounds **10** and **19** were compared, although their 4-chlorophenyl group is common, compound **19** was not as active as compound **10**. Another example that may be discussed from this view is 2,4-dichlorobenzyl carrying compound **17**. This is also having the same activity with compound **19** with a MIC value of 4 μg/ml. So, it may be asserted that both piperazine substituted phenyl ring and chloro substituted on the *para* position of the phenyl ring are important from the point of antidermatophytic activity. On the other hand, compound **22** bearing 4-bromophenyl and hydroxyl groups on the 4th position of the piperidine ring improved the expected activity of its chlorine bioisosteric analog, compound **23**. Compounds **15** and **16**, which were carrying inductive electron-donating methyl-substituted benzyl groups, were also among the most active compounds against *Trichophyton mentagrophytes var. erinacei* (MIC: 2 μg/ml). Unluckily, the decisive and definite influence on the in vitro antifungal activity could not be generated in terms of the electronegativity or the position of the substituent on the benzyl ring.

According to the cytotoxic effect studies on cell lines He-La (Human cervix epithelial carcinoma cell) and MRC-5 (human lung fibroblast cell), there was no selectivity between two groups. It can be seen that all the compounds were shown to be bioactive under non-toxic concentrations (≥128 μg/ml). Except for compounds **17**, **20**, and **21**, MNTCs of the compounds were higher (MNTCs: ≥128 μg/ml) than kojic acid (MNTCs: ≥256 μg/ml).

2.3 | Molecular modeling

To predict whether the compounds interact with binding sites of the targeted macromolecules, dermatophytes, we initially conducted a survey on the structure of proteins namely 14α-lanosterol demethylase, β-tubulin, chitin synthase, squalene epoxidase, β-1,3-glucan synthase in Protein Data Bank (PDB) (www.rcs.org) and found that there is no 3D crystallographic structure of mentioned proteins derived from *T. mentagrophytes, E. floccosum, and M. gypseum*. At this point, we oriented our molecular modeling efforts to the homology modeling concept.

Inspired by the partial similarity of the structures of griseofulvin and the synthesized compounds, we decided to run modeling studies with β-tubulin protein. Amino acid sequences of β-tubulin proteins of *T. mentagrophytes, E. floccosum, and M. gypseum* were incomplete in the protein sequence data bank. However, we could obtain the amino acids sequence of tubulin β-subunit of *T. rubrum* (TBB_TRIRU) with the accession code of Q5UBX3 as Fasta sequence from Uniprot Database. Since, *T. rubrum* and *T. mentagrophytes*, are the foremost pathogens as of dermatophyte fungi [26], homology modeling was used to build optimized 3D structure of the tubulin β-subunit of *T. rubrum*. The

TABLE 1 Antidermatophytic activity and cytotoxicity of the compounds **1–25** (MIC values as μg/ml)

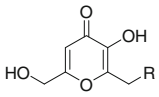

Comp. no.	R	Dermatophytes						*Cytotoxicity (MNTCs)*	
		Trichophyton mentagrophytes var. erinacei		Epidermophyton floccosum		Microsporum gypseum			
		NCPF 375	Isolated strain	RSKK 3027	Isolated strain	NCPF 580	Isolated strain	MRC-5	He-La
1	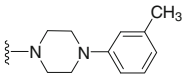	8	16	8	8	8	8	≥128	≥128
2	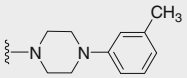	4	8	8	8	16	16	≥128	≥128
3	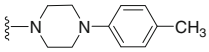	8	16	8	8	8	8	≥128	≥128
4[a]	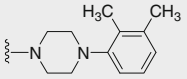	8	16	8	8	8	8	≥128	≥128
5[b]	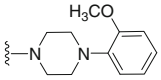	4	8	8	8	16	16	≥128	≥128
6[b]	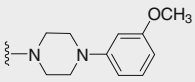	4	8	8	8	16	16	≥128	≥128
7	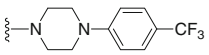	8	8	8	16	8	16	≥128	≥128
8[b]	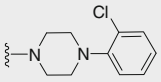	4	8	8	8	4	8	≥128	≥128
9[b]	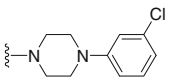	4	8	4	8	4	8	≥128	≥128
10[b]	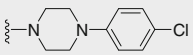	2	4	2	4	2	4	≥128	≥128
11[b]	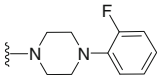	8	8	8	8	8	8	≥128	≥128
12[b]	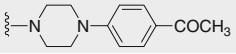	32	16	32	16	32	16	≥128	≥128
13	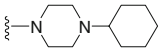	4	8	4	8	4	8	≥128	≥128
14	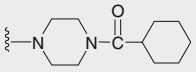	8	16	8	16	8	16	≥128	≥128
15	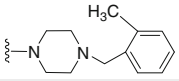	2	16	4	8	4	8	≥128	≥128
16	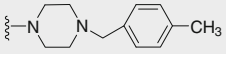	2	16	4	8	4	8	≥128	≥128
17	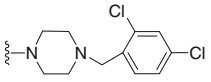	4	8	4	8	4	8	≥256	≥256

(Continues)

TABLE 1 (Continued)

Comp. no.	R	Dermatophytes						*Cytotoxicity (MNTCs)*	
		Trichophyton mentagrophytes var. erinacei		Epidermophyton floccosum		Microsporum gypseum			
		NCPF 375	Isolated strain	RSKK 3027	Isolated strain	NCPF 580	Isolated strain	MRC-5	He-La
18	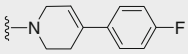	16	32	16	32	16	32	≥128	≥128
19[c]	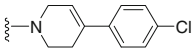	4	4	4	4	4	4	≥128	≥128
20	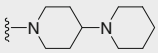	8	16	4	8	4	8	≥256	≥256
21[c]	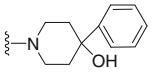	8	16	16	32	8	16	≥256	≥256
22[c]	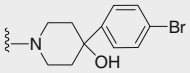	2	4	2	4	2	4	≥128	≥128
23[c]	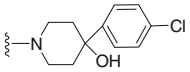	4	8	2	4	2	4	≥128	≥128
24[c]	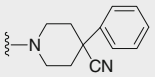	4	4	8	8	4	4	≥128	≥128
25[c]	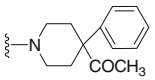	4	4	8	8	4	4	≥128	≥128
Kojic acid		4	4	4	4	2	2	≥256	≥256
Terbinafine		0.125	0.25	0.25	0.5	0.25	0.5		
Griseofulvin		0.5	1	0.5	1	0.5	1		
Itraconazole		0.25	0.5	0.125	0.25	0.125	0.25		

[a]Ref. [23].
[b]Ref. [22].
[c]Ref. [12].

model was generated using the SWISS-MODEL protein modeling tool and, after the structural check, it was used as the receptor for the molecular docking simulations.

The most active two compounds against dermatophytes, compound **10** and compound **22**, were selected for molecular modeling studies (Figure 3). It is worth mentioning that considering the ionization ratios of the compounds at physiological pH, the 1st atom of piperazine group of compound **10** and the 1st atom of piperidine group of compound **22** were kept as positively charged.

Docking results were evaluated meticulously. According to the docking results analysis, while 3-hydroxy substituent of 3-hydroxy-6-(hydroxymethyl)-4*H*-pyran-4-one ring of compound **10** forms hydrogen bond with Glu198, the protonated state of piperazine ring forms hydrogen bond with Ser314 amino acid residue.

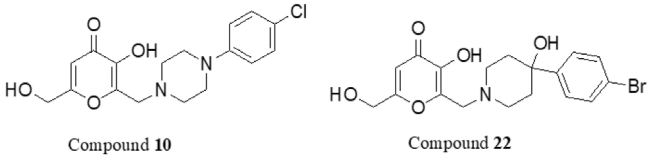

FIGURE 3 The most active compounds.

Compound **10** shows carbon hydrogen bonding interaction with Leu253. Furthermore, compound **10** makes pi-sigma pi-alkyl interactions with Leu246, Leu253, and Val368 amino acid residues.

As for compound **22**, the hydroxyl group of 4-(4-bromophenyl)-4-hydroxypiperidin-1-yl residue of compound **22** makes a hydrogen bond with Gln350. In addition, 4-oxo group of 3-hydroxy-6-(hydroxymethyl)-4*H*-pyran-4-one ring of compound **22** generates polar

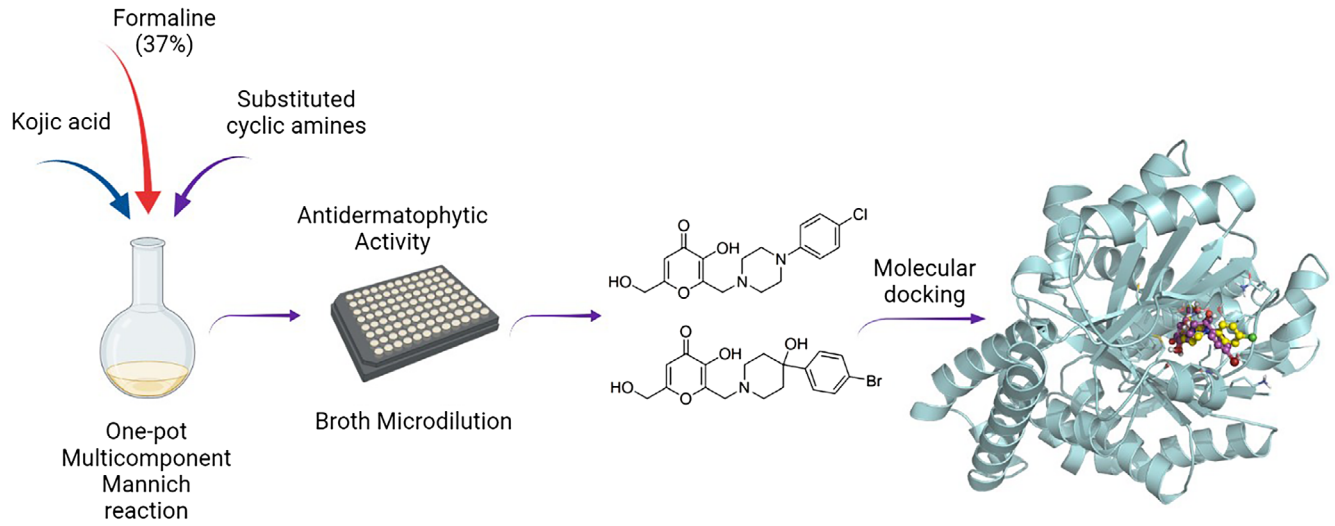

FIGURE 4 Compound 10 (yellow) and compound 22 (magenta) in the active site of β-tubulin protein.

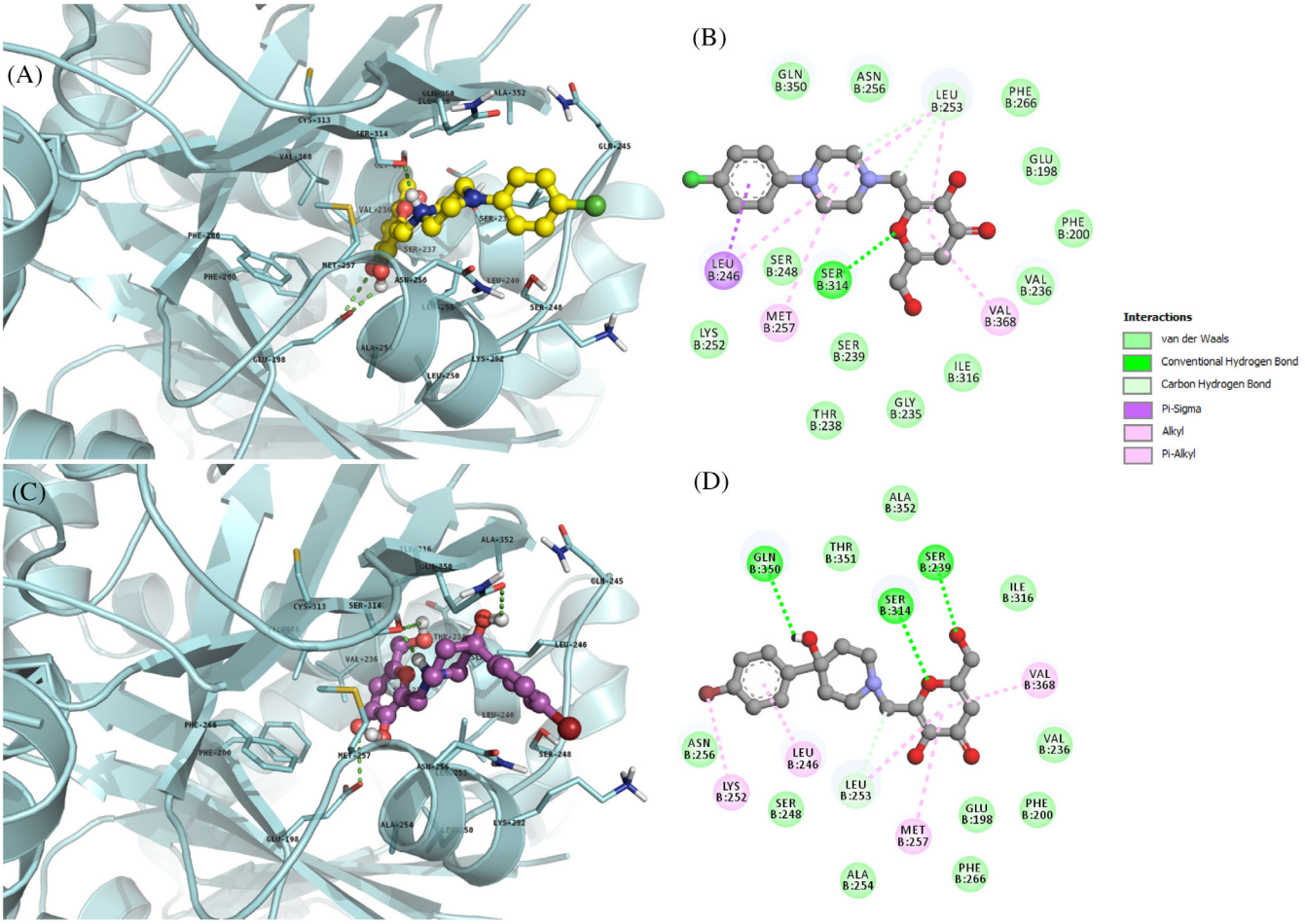

FIGURE 5 3D and 2D representations of molecular interactions between β-tubulin protein and compound **10** (A, B) and compound **22** (C, D).

contact with Glu198. Ser314 amino acid residue interacts with 6-hydroxymethyl substituent of 3-hydroxy-6-(hydroxymethyl)-4*H*-pyran-4-one ring and protonated state of piperidine ring. Compound **22** interacts with Leu253 by making a carbon hydrogen bonding interaction. Compound **22** makes alkyl and pi-alkyl interactions

with Leu246, Lys252, Met257, Ser314, and Val368 amino acid residues as well.

As whole protein view is shown with Figure 4, interactions between β-tubulin protein and compound **10** and compound **22** are visualized in Figure 5.

For 3D representations, amino acid residues within 5 Å of ligands are shown as sticks. Only polar hydrogens are visualized for clarity. Hydrogen bonds are depicted as green dashes. Compound **10** (yellow) and compound **22** (magenta) is presented with its ball and sticks form.

3 | CONCLUSION

In conclusion, to attempt novel antifungal agents carrying hydroxypyrone scaffold, Mannich bases of KA in the structure of 2-substituted-3-hydroxy-6-hydroxymethyl-4*H*-pyran-4-one were synthesized and screened for antidermatophyte effects with cytotoxic evaluation on He-La and MRC-5 cell line. Compound **10** and compound **22** showed the most potent activity against standard strains of all dermatophytes, exhibiting comparable effect with that of griseofulvin (MICs: 0.5–1.0 μg/ml) and terbinafine (MICs: 0.125–0.5 μg/ml) which are the most widely used agents for treating mycoses caused by dermatophytes. In addition, compounds **15** and **16** shared the same effect against *Trichophyton mentagrophytes var. erinacei* and compound **23** against *Microsporum gypseum* and *Epidermophyton floccosum* in broth microdilution assay in vitro. According to SAR analysis, halogen-containing piperazine derivatives were found to be more effective in antifungal activity. As of tested compounds, molecular docking studies of compound **10** and compound **22** with the homology model of β-tubulin protein revealed that hydroxypyrone ring has a high potential to make significant interactions such as hydrogen bonding. In the light of this study, further researches evaluating the anti-dermatophyte biofilm activity of similar agents will be carried out.

4 | EXPERIMENTAL SECTION

4.1 | Materials and methods

4.1.1 | Chemistry

All the chemicals used for the synthesis of the compounds were supplied by Merck (Darmstadt, Germany) and Aldrich Chemical Co. (Steinheim, Germany). Melting points were determined by a Thomas Hoover Capillary Melting Point Apparatus (Philadelphia, PA, USA) and were uncorrected. IR spectra were recorded on a Perkin Elmer FT IR-420 System, Spectrum BX spectrometer. ^{1}H NMR and ^{13}C NMR spectra were obtained with a Varian Mercury 400 MHz spectrophotometer in dimethylsulphoxide (DMSO-d_6). Tetramethylsilane (TMS) was used as an internal standard (chemical shift in δ, ppm). Mass spectral analysis was carried out with a Micromass ZQ LC–MS with Masslynx Software Version 4.1 by using the electrospray ionization (ESI+) method. The elemental analyses were performed with CHNS-932 (LECO) at the Ankara University Central Laboratory, Faculty of Pharmacy.

General synthetic route of Mannich reaction from kojic acid

Mannich bases were prepared by the reaction of substituted piperazine, tetrahydropyridine, or piperidine derivatives (0.01 mol) and kojic acid (0.01 mol) in methanol with 37% formaline. The mixture was stirred vigorously for 15 to 25 min. at room temperature. The resulting precipitate was collected by filtration and washed with cold methanol. The crude product was checked with thin layer chromatography (Mobile phase: Chloroform: MeOH, 9:1). Compounds 7, 13 and 14 were recrystallized from methanol whereas compounds 18 and 20 from ethanol.

*3-Hydroxy-6-(hydroxymethyl)-2-([4-o-tolylpiperazin-1-yl] methyl)-4H-pyran-4-one (**1**).* $C_{18}H_{22}N_2O_4$, M.W.: 330.39 g/mol; Yield: 68%; mp: 175–177 °C; %CHN Found (Calculated): C 65.42 (65.44), H 6.61 (6.71), N 8.38 (8.48); IR υ (cm^{-1}): 1609 (C=O, st), 1443 (C=C, st), 1195 (C-O, st); ^{1}H NMR (DMSO-d_6, 400 MHz) δ ppm: 2.22 (3H; s; Ar-CH_3), 2.61 (4H; brs; piperazine-H$^{2'}$, H$^{6'}$), 2.82 (4H; brs; piperazine-H$^{3'}$, H$^{5'}$), 3.59 (2H; s; -CH_2-), 4.32 (2H; s; HOCH_2-), 5.70 (2H; s; *H*OCH$_2$-), 6.34 (1H; s; H^5), 6.92–7.15 (4H; m; Ar-H); ^{13}CNMR (DMSO-d_6, 100 MHz) δ ppm: 18 (-*C*H$_3$), 52 (*C*-piperazine), 54 (*C*-piperazine), 54 (*C*-piperazine), 60 (*C*-piperazine), 109 (*C*H$_2$-OH), 119 (-*C*H = pyrone), 123 (*C*-Ar), 127 (*C*-Ar), 131 (*C*-Ar), 132 (*C*-Ar), 144 (*C*-Ar), 147 (*C*-Ar), 151 (=*C*-OH), 168 (-*C*-O), 174 (-*C*=O); ESI-MS (m/z): 331 (100%, M + H)$^+$, 353 (M + Na)$^+$.

*3-Hydroxy-6-(hydroxymethyl)-2-([4-m-tolylpiperazin-1-yl] methyl)-4H-pyran-4-one (**2**).* $C_{18}H_{22}N_2O_4$, M.W.: 330.39 g/mol; Yield: 80%; mp: 188–189 °C; %CHN Found (Calculated): C 65.20 (65.44), H 6.90 (6.71), N 8.59 (8.48); IR υ (cm^{-1}): 1610 (C=O, st), 1456 (C=C, st), 1200 (C-O, st); ^{1}H NMR (DMSO-d_6, 400 MHz) δ ppm: 2.19 (3H; s; -CH_3), 2.60 (4H; t; J = 4.8; piperazine-H$^{2'}$, H$^{6'}$), 3.06 (4H; t; J = 4.8; piperazine-H$^{3'}$,H$^{5'}$), 3.58 (2H; s; -CH_2-), 4.31 (2H; s; HOCH_2-), 6.55 (1H; s; H^5), 6.8–7.01 (4H; m; Ar-H$^{2''}$, H$^{6''}$), 9.03 (1H; s; -O*H*); ^{13}CNMR (DMSO-d_6,

100 MHz) δ ppm: 19.90 (-CH_3), 48.54 (-CH_2), 52.35 (-*C*-piperazine), 53.46 (*C*-piperazine), 59.53 (*C*-piperazine), 108.86 (-*C*H), 115.6 (-*C*H), 129.22 (-*C*H), 127.54 (*C*-Ar), 143.65 (*C*-pyrone), 146.29 (=*C*-OH), 148.81 (*C*-Ar), 167.55 (-*C*-O), 173.51 (-*C*=O); ESI-MS 177 (% 100), 331 $(M + H)^+$, 353 $(M + Na)^+$.

*3-Hydroxy-6-(hydroxymethyl)-2-([4-p-tolylpiperazin-1-yl]methyl)-4H-pyran-4-one (**3**).* $C_{18}H_{22}N_2O_4$, M.W.: 330.39 g/mol; Yield: 87%; mp: 186–187 °C; %CHN Found (Calculated): C 65.05 (65.44), H 6.85 (6.71), N 8.41 (8.48); IR υ (cm^{-1}): 1610 (C=O, st), 1456 (C=C, st), 1200 (C-O, st); ^{1}H NMR (DMSO-d_6, 400 MHz) δ ppm: 2.19 (3H; s; Ar-CH_3), 2.50–2.60 (4H; brs; piperazine-H$^{2'}$, H$^{6'}$), 3.04–3.06 (4H; brs; piperazine-H$^{3'}$, H$^{5'}$), 3.57 (2H; s; -CH_2-), 4.31 (2H; s; HOCH_2-), 5.70 (2H; s; *H*OCH$_2$-), 6.34 (1H; s; H^5), 6.81 (2H; d; *J* = 8.40; Ar- H$^{2''}$, H$^{6''}$), 7.01 (2H; d; *J* = 8.40; Ar- H$^{3''}$, H$^{5''}$), 9.06 (1H; brs; pyrone-O*H*); ^{13}CNMR (DMSO-d_6, 100 MHz) δ ppm: 21 (-CH_3), 49 (*C*-piperazine), 53 (*C*-piperazine), 54 (*C*-piperazine), 60 (*C*-piperazine), 109 (CH_2-OH), 116 (-*C*H = pyrone), 128 (*C*-Ar), 130 (*C*-Ar), 144 (*C*-Ar), 147 (*C*-Ar), 151 (=*C*-OH), 168 (-*C*-O), 174 (-*C*=O); ESI-MS (m/z):177 (100%), 331 $(M + H)^+$, 353 $(M^+ + Na)^+$.

*2-((4-[2,3-Dimethylphenyl]piperazine-1-yl)methyl)-3-hydroxy-6-(hydroxymethyl)-4H-pyran-4-one (**4**) [23].* $C_{19}H_{24}N_2O_4$, M.W.: 344.40 g/mol; Yield: 80%; mp: 187–188 °C; %CHN Found (Calculated): C 66.29 (66.26), H 7.05 (7.02), N 8.07 (8.13); IR υ (cm^{-1}): 1609 (C=O, st), 1448 (C=C, st), 1192 (C-O, st); ^{1}H NMR (DMSO-d_6, 400 MHz) δ ppm: 2.13 (3H; s; Ar-CH_3), 2.19 (3H; s; -Ar-CH_3), 2.60–2.78 (8H; brs; piperazin-*H*) 3.58 (2H; s; -CH_2-), 4.32 (2H; s; HOCH_2-), 5.70 (2H; s; *H*OCH$_2$-), 6.34 (1H; s; H^5), 6.85–7.04 (3H; brs; Ar-*H*), 9.07 (1H; brs; pyranone-O*H*); ^{13}CNMR (DMSO-d_6, 100 MHz) δ ppm: 14 (-CH_3), 21 (-CH_3), 52 (*C*-piperazine), 54 (*C*-piperazine), 54 (*C*-piperazine), 60 (*C*-piperazine), 109 (CH_2-OH), 117 (-*C*H = pyrone), 125 (*C*-Ar), 126 (*C*-Ar), 131 (*C*-Ar), 138 (*C*-Ar), 144 (*C*-Ar), 147 (*C*-Ar), 151 (=*C*-OH), 168 (-*C*-O), 174 (-*C*=O); ESI-MS (m/z): 177 (100%), 345 $(M + H)^+$, 367 $(M + Na)^+$.

*3-Hydroxy-6-(hydroxymethyl)-2-((4-(4-[trifluoromethyl]phenyl)piperazine-1-yl)methyl)-4H-pyran-4-one (**7**).* $C_{18}H_{19}F_3N_2O_4$, M.W.: 384.36 g/mol; Yield: 70%; mp: 181–182 °C; %CHN Found (Calculated): C 55.86 (56.25), H 5.06 (4.98), N 7.30 (7.29); IR υ (cm^{-1}): 1614 (C=O, st), 1462 (C=C, st), 1201 (C-O, st); ^{1}H NMR (DMSO-d_6, 400 MHz) δ ppm: 2.60 (4H; t; *J* = 4.80; piperazine-H$^{2'}$, H$^{6'}$), 3.27 (4H; t; *J* = 5.0; piperazine-H$^{3'}$, H$^{5'}$), 3.58 (2H; s; -CH_2-), 4.31 (2H; s; HOCH_2-), 5.70 (2H; s; *H*OCH$_2$-), 6.34 (1H; s; H^5), 7.05 (2H; d; *J* = 8.80; Ar-H$^{2''}$, H$^{6''}$), 7.49 (2H; d; *J* = 8.80; Ar-H$^{3''}$, H$^{5''}$), 9.08 (1H; brs; pyranone-O*H*); ^{13}CNMR (DMSO-d_6, 100 MHz) δ ppm: 48 (*C*-piperazine), 53 (*C*-piperazine), 54 (*C*-piperazine), 60 (*C*-piperazine), 109 (CH_2-OH), 114 (-*C*H = pyrone), 118 (*C*-Ar), 119 (*C*-Ar), 124 (*C*-Ar), 125 (*C*-Ar), 127 (CF_3), 144 (*C*-Ar), 147 (*C*-Ar), 154 (=*C*-OH), 168 (-*C*-O), 174 (-*C*=O); ESI-MS (m/z): 177 (100%), 385 $(M + H)^+$, 407 $(M + Na)^+$.

*2-([4-Cyclohexylpiperazin-1-yl]methyl)-3-hydroxy-6-(hydroxymethyl)-4H-pyran-4-one (**13**).* $C_{17}H_{26}N_2O_4$, M.W.: 322.40 g/mol; Yield: 65%; mp: 198–199 °C; %CHN Found (Calculated): C 63.12 (63.33), H 7.73 (8.13), N 8.77 (8.69); IR υ (cm^{-1}): 1605 (C=O, st), 1444 (C=C, st), 1203 (C-O, st); ^{1}H NMR (DMSO-d_6, 400 MHz) δ ppm: 1.12–1.20 (5H; m; cyclohexyl); 1.5 (1H; d; cyclohexyl); 1.70–1.73 (4H; m; cyclohexyl); 2.10–2.20 (1H; brs; cyclohexyl); 2.43–2.51 (8H; m; piperazine), 3.48 (2H; s; -CH_2), 4.29 (2H; s; -CH_2OH), 5.67 (1H; brs; -CH$_2$O*H*); 6.31 (1H; s; *H*^{5}); ^{13}CNMR (DMSO-d_6, 100 MHz) δ ppm: 25.05 (-CH_2), 25.10 (-CH_2), 25.83 (-CH_2), 48.30 (-CH_2), 59.50 (-CH_2), 62.30 (-*C*H), 108.92 (-*C*H), 143.24 (-*C*-pyrone), 146.58 (-*C*-pyrone), 167.53 (-*C*-pyrone), 173.54 (-*C*-pyrone); ESI-MS (m/z): 323 (100%, M + H)$^+$, 345 $(M + Na)^+$.

*2-((4-[Cyclohexanecarbonyl]piperazine-1-yl)methyl)-3-hydroxy-6-(hydroxymethyl)-4H-pyran-4-one (**14**).* $C_{18}H_{26}N_2O_5$, M.W.: 350.41 g/mol; Yield: 62%; mp: 184–185 °C; %CHN Found (Calculated): C 61.60 (61.20), H 7.27 (7.48), N 8.01 (7.99); IR υ (cm^{-1}): 1654 (C=O, st), 1456 (C=C, st), 1051 (C-O, st); ^{1}H NMR (DMSO-d_6, 400 MHz) δ ppm: 1.19–0.1.29 (6H; m; cyclohexyl), 1.56–1.66 (5H; m; cyclohexyl), 2.35–2.50 (8H; m; piperazine), 3.40–3.50 (2H; d; -CH_2OH), 4.27 (2H; s; -CH_2), 5.64 (1H; brs; -CH$_2$O*H*); 6.30 (1H; s; *H*^{5}), 8.97 (1H; brs; pyrone-O*H*); ^{13}CNMR (DMSO-d_6, 100 MHz) δ ppm: 25.04 (-CH_2), 25.47 (-CH_2), 29.03 (-CH_2), 38.85 (-CH_2), 40.80 (-CH_2), 44.60 (-CH_2), 52.44 (-CH_2), 52.87 (-CH_2), 53.33 (-CH_2), 59.49 (-CH_2), 108.84 (-*C*H), 143.64 (-*C*-pyrone), 146.15 (-*C*-pyrone), 167.55 (-*C*-pyrone), 173.20 (-*C*-carbonyl) 173.49; ESI-MS (m/z): 351 (100%, M + H)$^+$, 373 $(M + Na)^+$.

*2-((4-[2-Methylbenzyl]piperazine-1-yl)methyl)-3-hydroxy-6-(hydroxymethyl)-4H-pyran-4-one (**15**).* $C_{19}H_{24}N_2O_4$, M.W.: 344.40 g/mol; Yield: 77%; mp: 185–186 °C; %CHN Found (Calculated): C 65.28 (66.26), H 6.81 (7.02), N 8.40 (8.13); IR υ (cm^{-1}): 1597 (C=O, st), 1448 (C=C, st), 1187 (C-O, st); ^{1}H NMR (DMSO-d_6, 400 MHz) δ ppm: 2.29 (3H; s; -CH_3), 2.51 (8H; brs; piperazine), 3.39 (2H; s; -CH_2-), 3.50 (2H; s; -CH_2phenyl), 4.29 (2H; s; -CH_2OH), 5.66 (1H; brs; -CH$_2$O*H*); 6.31 (1H; s; *H*^{5}), 7.1–7.2 (4H; m; Ar-*H*); 8.94 (1H; brs; -O*H*); ^{13}CNMR (DMSO-d_6, 100 MHz) δ ppm: 18.78 (-CH_3), 52.57 (*C*-piperazine), 53.57 (*C*-piperazine), 59.56 (*C*-piperazine), 59.99 (*C*-piperazine), 108.92 (CH_2-OH), 125.34 (-*C*H = pyrone), 126.84 (-*C*H), 129.43 (-*C*H),

130.00 (-*C*H), 136.24 (*C*-Ar), 136.94 (*C*-Ar), 143.63 (*C*-pyrone), 146.53 (=*C*-OH), 167.55 (-*C*-O), 173.55 (-*C*=O); ESI-MS (m/z): 345 (M + H, % 100)$^+$, 367 (M + Na)$^+$.

*2-((4-[4-Methylbenzyl]piperazine-1-yl)methyl)-3-hydroxy-6-(hydroxymethyl)-4*H*-pyran-4-one (**16**).* $C_{19}H_{24}N_2O_4$, M.W.: 344.40 g/mol; Yield: 82%; mp: 198–199 °C; %CHN Found (Calculated): C 66.18 (66.26), H 7.24 (7.02), N 8.24 (8.13); IR υ (cm^{-1}): 1609 (C=O, st), 1455 (C=C, st), 1198 (C-O, st); ^{1}H NMR (DMSO-d_6, 400 MHz) δ ppm: 2.27 (3H; s; -CH_3), 2.45 (4H; brs; piperazine-$H^{2'}$, $H^{6'}$), 2.50 (4H; brs; piperazine-$H^{3'}$, $H^{5'}$), 3.39 (2H; s; -CH_2-), 3.50 (2H; s; -CH_2-phenyl), 4.28 (2H; s; -CH_2OH), 5.59 (1H; brs; -CH$_2$O*H*); 6.30 (1H; s; H^5), 6.09 (2H; d; J = 8; Ar-$H^{2''}$, $H^{6''}$), 7.15 (2H; d; J = 7.6; Ar-$H^{3''}$, $H^{5''}$); ^{13}CNMR (DMSO-d_6, 100 MHz) δ ppm: 20.57 (-CH_3), 52.35 (-CH_2), 53.53 (-CH_2), 59.56 (-CH_2), 61.63 (-CH_2), 108.89 (-C*H*), 128.61 (-C*H*), 134.98 (*C*-Ar), 135.76 (*C*-Ar), 143.52 (*C*-pyrone), 146.49 (=*C*-OH), 167.43 (-*C*-O), 173.46 (-*C*=O); ESI-MS (m/z): 345 (M + H, % 100)$^+$, 367 (M + Na)$^+$.

*2-((4-[2,4-Dichlorobenzyl]piperazine-1-yl)methyl)-3-hydroxy-6-(hydroxymethyl)-4*H*-pyran-4-one (**17**).* $C_{18}H_{20}Cl_2N_2O_4$, M.W.: 399.27 g/mol; Yield: 61%; mp: 184–185 °C; %CHN Found (Calculated): C 53.77 (54.15), H 5.11 (5.05), N 7.36 (7.02); IR υ (cm^{-1}): 1617 (C=O, st), 1467 (C=C, st), 1195 (C-O, st); ^{1}H NMR (DMSO-d_6, 400 MHz) δ ppm: 2.41–2.44 (4H; brs; piperazine-$H^{2'}$, $H^{6'}$), 2.47–2.49 (4H; brs; piperazine-$H^{3'}$, $H^{5'}$), 3.49 (4H; s; -CH_2-), 4.27 (2H; d; J = 2.80; HOCH_2-), 5.65 (1H; brs; *H*OCH$_2$-), 6.29 (1H; s; H^5), 7.37 (1H; dd; J = 8.00, J = 2.40; Ar- $H^{5''}$), 7.46 (1H; d; J = 8.80; Ar-$H^{6''}$), 7.55 (1H; d; J = 2.00; Ar-$H^{3''}$), 8.99 (1H; brs; pyranone-O*H*); ^{13}CNMR (DMSO-d_6, 100 MHz) δ ppm: 53 (*C*-piperazine), 53 (*C*-piperazine), 54 (*C*-piperazine), 59 (*C*-piperazine), 60 (-CH_2), 109 (CH_2-OH), 127 (-C*H* = pyrone), 129 (*C*-Ar), 132 (*C*-Ar), 134 (*C*-Ar), 135 (*C*-Ar), 144 (*C*-Ar), 147 (*C*-Ar), 168 (-*C*-O), 174 (-*C*=O); ESI-MS (m/z): 177 (100%), 400 (M + H)$^+$, 422 (M + Na)$^+$.

*2-((4-(4-Fluorophenyl)-5,6-dihydropyridine-1(2*H*)-yl)methyl)-3-hydroxy-6-(hydroxymethyl)-4*H*-pyran-4-one (**18**).* $C_{18}H_{18}FNO_4$, M.W.: 331.34 g/mol; Yield: 70%; mp: 192–193 °C; %CHN Found (Calculated): C 64.86 (65.25), H 5.43 (5.48), N 4.23 (4.23); IR υ (cm^{-1}): 1607 (C=O, st), 1456 (C=C, st), 1197 (C-O, st); ^{1}H NMR (DMSO-d_6, 400 MHz) δ ppm: 2.51 (2H; brs; pyridine), 2.72 (2H; t; J = 5.60; pyridine), 3.15 (2H; d; J = 2.80; pyridine), 3.36 (1H; brs; pyridine), 3.64 (2H; s; -CH_2-), 4.31 (2H; s; HOCH_2-), 5.71 (2H; brs; *H*OCH$_2$-), 6.10 (1H; s; =C*H*-C = pyridine), 6.34 (1H; s; H^5), 7.05 (2H; t; J = 6.80; Ar-$H^{2''}$, $H^{6''}$), 7.49 (2H; t; J = 7.30; Ar-$H^{3''}$, $H^{5''}$), 9.09 (1H; brs; pyranone-O*H*); ^{13}CNMR (DMSO-d_6, 100 MHz) δ ppm: 28 (*C*-pyridine), 50 (*C*- pyridine), 53 (*C*- pyridine), 54 (*C*- pyridine), 60 (-CH_2), 109 (CH_2-OH), 116 (*C*-Ar), 122 (*C*-Ar), 127 (*C*-Ar), 134 (*C*-Ar), 144 (*C*-Ar), 147 (*C*-Ar), 160 (-C*H* = pyrone), 163 (-*C* = pyrone), 168 (-*C*-O), 174 (-*C*=O); ESI-MS (m/z): 177 (100%), 332 (M + H)$^+$, 354 (M + Na)$^+$.

*2-((4-[Piperidin-1-yl]piperidine-1-yl)methyl)-3-hydroxy-6-(hydroxymethyl)-4H-pyran-4-one (**20**).* $C_{17}H_{26}N_2O_5$, M.W.: 322.40 g/mol; Yield: 60%; mp: 187–189 °C; %CHN Found (Calculated): C 62.92 (63.33), H 8.08 (8.13), N 8.76 (8.69); IR υ (cm^{-1}): 1605 (C=O, st), 1445 (C=C, st), 1110 (C-O, st); ^{1}H NMR (DMSO-d_6, 400 MHz) δ ppm: 1.36–1.46 (8H; m; piperidine); 1.65 (2H; d; piperidine); 2.03 (2H; t; piperidine); 2.2 (1H; brs; piperidine); 2.50 (4H; t; piperidine); 2.85 (2H; d; piperidine), 3.47 (2H; s; -CH_2), 4.29 (2H; s; -CH_2OH), 5.5–5.8 (1H; brs; -CH$_2$O*H*); 6.31 (1H; s; H^5) ^{13}CNMR (DMSO-d_6, 100 MHz) δ ppm: 24.28 (-CH_2), 25.77 (-CH_2), 27.20 (-CH_2), 49.53 (-C*H*), 52.53 (-CH_2), 53.57 (-CH_2), 59.48 (-CH_2), 108.82 (-C*H*), 143.47 (-*C*-pyrone), 146.70 (-*C*-pyrone), 167.43 (-*C*-pyrone), 173.45 (-*C*-pyrone); ESI-MS (m/z): 323(100%, M + H)$^+$, 345 (M + Na)$^+$.

4.1.2 | Antidermatophytic assays

Compounds **1–25** were dissolved in dimethylsulphoxide (3%) and *d*-H$_2$O at a final concentration of 512 μg/ml and sterilized by filtration using 0.22 μm Millipore (MA 01730, USA), and used as the stock solutions. Terbinafine, griseofulvin, and itraconazole were used as the standard antifungal drugs. Reference pharmaceutical agents were purchased from Sigma Chemical Co. (St. Louis, MO, USA) and dissolved in dimethylsulphoxide or *d*-water. The stock solutions of the agents were prepared in a medium, according to the Clinical and Laboratory Standards Institute [16, 17].

Antidermatophytic activity tests were carried out against standard (ATCC; American type culture collection, RSKK; Culture collection of Refik Saydam Central Hygiene Institute; NCPF; National Collection of Pathogenic Fungi) and isolated strains (clinical isolate obtained from Department of Microbiology, Faculty of Medicine, Gazi University). Mueller Hinton Broth (MHB; Difco) and Mueller Hinton Agar (MHA; Oxoid) were applied for growing and diluting of the bacterial suspensions. The dermatophytic fungi species used were *Microsporum gypseum* (NCPF580), *Trichophyton mentagrophytes var. erinacei* (NCPF375), and *Epidermophyton floccosum* (RSKK3027) were included as quality control strains. Dermatophytes were subcultured onto potato dextrose agar (PDA) plates at 28 °C, for 7–14 days. The broth

microdilution method was used for antifungal activity tests. The media was placed into every 96 wells of the microplates. Extract solutions at 512 μg/ml were added into first rows of microplates, and twofold dilutions of the compounds (256–0.125 μg /ml) were made by dispensing the solutions to the remaining wells. 10 μl culture suspensions were inoculated into all the wells. All organisms were tested in triplicate in each run of the experiments. The sealed microplates were incubated at 35°C for 24 h and 48 h in a humid chamber. DMSO, H_2O, pure microorganisms, and pure media were used as control wells. The lowest concentration of the extracts that completely inhibit macroscopic growth was determined, and minimum inhibitory concentrations (MICs) were reported as described in a previous study [16, 17]. The MIC of each extract was determined by using broth microdilution techniques as described by CLSI for filamentous fungi [17]. The medium was RPMI 1640 broth with l-glutamine and buffered to pH 7.0 with 0.165 M MOPS buffer (3-[*N*-morpholino]propane sulfonic acid; 34.54 g/L) but without sodium bicarbonate (Sigma-Aldrich, Germany), sterilized by filtration. A sterile 96 well microdilution plates were prepared and stored at −70°C until use. Rows from 2 to 12 contained the series of test materials dilutions concentrations ranging from 0.0625 to 128 μg/ml in 100 μl a volume and inoculated with 100 μl inoculum suspensions using a multichannel pipette. For each test plate, two drug-free controls were included, one with the medium alone (sterility control) and the other with medium-plus inoculum suspension, which was served as the growth control. Tests were performed in triplicate. Each well was inoculated with 100 μl of the corresponding inoculums and incubated at 28°C for 7 days. The microplates were read visually with the aid of an inverted reading mirror after 7 days for dermatophytes.

4.1.3 | Cytotoxicity assay

The culture of the cells (MRC-5, He-La) was grown in EMEM (Eagle's Minimal Essential Medium; Seromed; Biochrom; Berlin; Germany) enriched with 10% fetal calf serum (Biochrom, Germany), 100 mg/ml of streptomycin and 100 IU/ml of penicillin in a humidified atmosphere of 5% carbon dioxide (CO_2) at 37°C. The cells were harvested using trypsin solution (BibcoLife Technologies, UK). MNTCs of each sample was determined by the method described previously [17] based on cellular morphologic alteration. Several concentrations of each sample were placed in contact with confluent cell monolayers and incubated in 5% CO_2 at 37 °C for 48 h. After the incubation period, drug concentrations that were not toxic to viable cells were evaluated as nontoxic and compared with nontreated cells for validation. The rows that cause damage in all cells were evaluated as toxicity in the present concentration. Besides, maximum drug concentrations that did not affect the cells were evaluated as nontoxic concentration. MNTCs were determined by comparing treated and controlling untreated cultures.

4.1.4 | Modeling studies

Homology model was built with SWISS-MODEL protein modeling tool (http://www.swissmodel.expasy.org). Template was selected based on higher identity toward sequence of tubulin β-subunit of *T. rubrum* with Q5UBX3 Fasta sequence (TBB_TRIRU) (https://www.uniprot.org/). PDB (http://www.rcsb.org/) structure of 5CA1 with 2.40 Å was selected as the model template with acceptable model parameters and 97% coverage.

The generated 3D structure of the model protein was checked by SAVES online server tool (https://saves.mbi.ucla.edu/). After the structural check, the generated model was used as the receptor for the molecular docking simulations.

BIOVIA Discovery Studio Visualizer and AutoDock Tools were used for the preparation of compounds **10** and **22**. As the 1st atom of piperazine group of compound **10**, as well as the 1st atom of piperidine group of compound **22**, were expected to be protonated, structures were prepared accordingly.

Docking calculations were executed with Autodock Vina [27] and evaluated with PyMOL. Docked poses of the most active two compounds in β-tubulin model were visualized in Figure 5.

ACKNOWLEDGMENTS

This work was financially supported by a research grant provided by the Foundation for Scientific Research Projects of Gazi University (Project code no: 02/2011-35) and TUBITAK (Project no.: SBAG113S527). Images in Figure 1 and Graphical Abstract were created in BioRender.com application.

DATA AVAILABILITY STATEMENT

The data that support the findings of this study are available from the corresponding author upon reasonable request.

ORCID

Gülşah Karakaya https://orcid.org/0000-0002-3827-7537

REFERENCES

[1] L. A. Soares, J. C. O. Sardi, F. P. Gullo, N. S. Pitangui, L. Scorzoni, F. S. Leite, M. S. M. Giannini, A. M. F. Almeida, *Braz. J. Microb.* **2013**, *44*(4), 1035.

[2] T. R. Jacob, N. T. A. Peres, M. P. Martins, E. A. S. Lang, P. R. Sanches, A. Rossi, N. M. Martinez-Rossi, *Front. Microbiol.* **2015**, *6*, 1241.

[3] N. T. Peres, F. C. Maranhão, A. Rossi, N. M. Martinez-Rossi, *An. Bras. Dermatol.* **2010**, *85*, 657.

[4] P. Nenoff, C. Krüger, G. Ginter-Hanselmayer, H. J. Tietz, *J. Dtsch. Dermatol. Ges.* **2014**, *12*(3), 188.

[5] S. Gnat, D. Lagowski, A. Nowakiewicz, *J. App. Microbiol.* **2020**, *129*, 212.

[6] N. M. Martinez-Rossi, T. A. Bitencourt, N. T. A. Peres, E. A. S. Lang, E. V. Gomes, N. R. Quaresemin, M. P. Martins, L. Lopes, A. Rossi, *Front. Microbiol.* **2018**, *9*, 1108.

[7] S. Campoy, J. L. Adrio, *Biochem. Pharmacol.* **2017**, *133*, 86.

[8] J. Brtko, L. Rondahl, M. Fickova, D. Hudecova, V. Eybl, M. Uher, *Centr. Eur. J. Publ. Health* **2004**, *12*, S16.

[9] H. Mitani, I. Koshiishi, T. Sumita, T. Imanari, *Eur. J. Pharmacol.* **2001**, *411*, 169.

[10] M. D. Aytemir, B. Ozcelik, *Eur. J. Med. Chem.* **2010**, *45*, 4089.

[11] M. D. Aytemir, U. Calis, M. Ozalp, *Arch. Pharm.* **2004**, *337*, 281.

[12] M. D. Aytemir, U. Calis, *Arch. Pharm.* **2010**, *343*, 173.

[13] Y. Higa, M. Kawabe, K. Nabae, Y. Toda, S. Kitamoto, T. Hara, N. Tanaka, K. Kariya, M. Takahashi, *J. Toxicol. Sci.* **2007**, *32*, 143.

[14] G. Karakaya, A. Ercan, S. Oncul, M. D. Aytemir, *Anti-Cancer. Agent. Me.* **2018**, *18*, 2137.

[15] X. Xiong, M. C. Pirrung, *Organic Lett.* **2008**, *10*, 1151.

[16] G. Karakaya, M. D. Aytemir, B. Özçelik, Ü. Calış, *J. Enzyme Inhib. Med. Chem.* **2013**, *28*(3), 627.

[17] M. D. Aytemir, B. Ozçelik, G. Karakaya, *Bioorg. Med. Chem. Lett.* **2013**, *23*(12), 3646.

[18] M.D. Aytemir, B. Ozcelik, I.E. Orhan, G. Karakaya, F.S. Senol (**2018**). US Patent 2017–0197946, filled May 17, 2016, issued July 13, 2018.

[19] S. B. Ozdemir, Y. U. Cebeci, H. Bayrak, A. Mermer, Ş. Ceylan, A. Demirbas, Ş. A. Karaoglu, N. Demirbas, *Heterocyclic Commun.* **2017**, *23*(1), 43.

[20] X. Zhang, P. Lei, T. Sun, X. Jin, X. Yang, Y. Ling, *Molecules* **2017**, *22*(12), 2085.

[21] N. Mohsin, M. Ahmad, *Turk. J. Chem.* **2018**, *42*, 1191.

[22] M. D. Aytemir, E. Septioğlu, U. Caliş, *Arzneimittelforschung.* **2010**, *60*(1), 22.

[23] D.S. Goldfarb (**2014**). US Patent 2009–0163545, filled Dec 22, 2008, issued June 25, 2009.

[24] H. Wu, Y. Shen, L. Y. Fan, Y. Wan, P. Zhang, C. Chen, W. Wang, *Tetrahedron* **2007**, *63*, 2404.

[25] F. O. Pereira, *Med. Mycol.* **2021**, *59*(4), 313.

[26] R. Gaziano, E. Campione, F. Iacovelli, D. Marino, F. Pica, P. Di Francesco, S. Aquaro, F. Menichini, M. Falconi, L. Bianchi, *Drug. Des. Devel. Ther.* **2018**, *12*, 2185.

[27] O. Trott, A. J. Olson, *J. Comput. Chem.* **2010**, *31*(2), 455.

SUPPORTING INFORMATION

Additional supporting information may be found in the online version of the article at the publisher's website.

How to cite this article: G. Karakaya, A. Türe, A. Özdemir, B. Özçelik, M. Aytemir, *J. Heterocycl. Chem.* **2022**, *59*(10), 1801. https://doi.org/10.1002/jhet.4520